Multiple Univariate Data Analysis Reveals the Inulin Effects on the High-Fat-Diet Induced Metabolic Alterations in Rat Myocardium and Testicles in the Preobesity State

ARTICLE *in* JOURNAL OF PROTEOME RESEARCH · MAY 2013

Impact Factor: 4.25 · DOI: 10.1021/pr400341f · Source: PubMed

Journal of proteome research

Article

pubs.acs.org/jpr

Multiple Univariate Data Analysis Reveals the Inulin Effects on the High-Fat-Diet Induced Metabolic Alterations in Rat Myocardium and Testicles in the Preobesity State

Yixuan Duan,[†,‡] Yanpeng An,[§,‡] Ning Li,[§,‡] Bifeng Liu,[†] Yulan Wang,[‡] and Huiru Tang*[,‡]

[†]Britton Chance Center for Biomedical Photonics at Wuhan National Laboratory for Optoelectronics—Hubei Bioinformatics and Molecular Imaging Key Laboratory, Systems Biology Theme, Department of Biomedical Engineering, College of Life Science and Technology, Huazhong University of Science and Technology, Wuhan 430074, P. R. China

[‡]Key Laboratory of Magnetic Resonance in Biological Systems, State Key Laboratory of Magnetic Resonance and Atomic and Molecular Physics, Centre for Biospectroscopy and Metabonomics, Wuhan Institute of Physics and Mathematics, the Chinese Academy of Sciences, Wuhan 430079, P. R. China

[§]University of Chinese Academy of Sciences, Beijing 100049, P. R. China

S *Supporting Information*

ABSTRACT: Obesity is a worldwide epidemic and a well-known risk factor for many diseases affecting billions of people's health and well-being. However, little information is available for metabolic changes associated with the effects of obesity development and interventions on cardiovascular and reproduction systems. Here, we systematically analyzed the effects of high-fat diet (HFD) and inulin intake on the metabolite compositions of myocardium and testicle using NMR spectroscopy. We developed a useful high-throughput method based on multiple univariate data analysis (MUDA) to visualize and efficiently extract information on metabolites significantly affected by an intervention. We found that HFD caused widespread metabolic changes in both rat myocardium and testicles involving fatty acid β-oxidation together with the metabolisms of choline, amino acids, purines and pyrimidines even before HFD caused significant body-weight increases. Inulin intake ameliorated some of the HFD-induced metabolic changes in both myocardium (3-HB, lactate and guanosine) and testicle tissues (3-HB, inosine and betaine). A remarkable elevation of *scyllo*-inositol was also observable with inulin intake in both tissues. These findings offered essential information for the inulin effects on the HFD-induced metabolic changes and demonstrated this MUDA method as a powerful alternative to traditionally used multivariate data analysis for metabonomics.

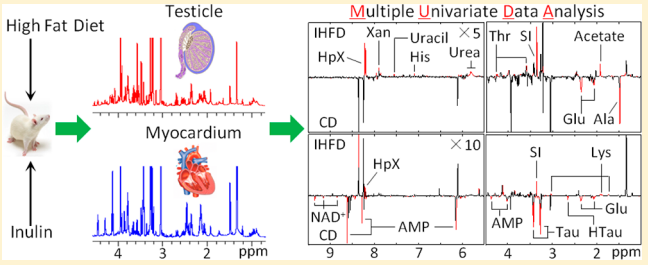

KEYWORDS: *high-fat diet, inulin, metabonomics, MUDA, myocardium, reproductive system*

INTRODUCTION

Obesity is now becoming an epidemic affecting billions of people's health and well being in both the developed and developing countries. Data from National Center for Health Statistics showed that 35.7% of U.S. adults were obese in 2009−2010[1] with the associated costs mounting to 200 billion U.S. dollars annually.[2] It was even more alarming that 16.9% of U.S. children and adolescents were obese in 2009−2010 with prevalence increasing especially among boys. Similar problems are occurring in the developing countries as well. For example, in China alone, about 200 million people were obese or overweight in 2007 and this number was rising rapidly.[2] Obesity has also been proved to be a serious risk factor for a number of diseases including hypertension,[3] diabetes,[4] cardiovascular,[5,6] and reproductive system diseases.[7,8]

Therefore, extensive researches have been focused on the obesity development[9,10] and therapies for treatments.[11,12] It is now known that both genetic and environmental factors, such as high-fat diets and lack of exercise, are important for the development of obesity. Animal models are well established to study the mechanistic aspects of obesity development[13] and long-term high-fat diet (HFD) has been shown to cause comprehensive transcriptomic variations in the rat liver involving multiple metabolic pathways together with the inflammation and stress responses.[14] In particular, PPARα, carnitine palmitoyltransferase 1, and 3-hydroxy-3-methylglutaryl−coenzyme A reductase were down-regulated, whereas lipogenesis transcription factor Srebf1 and stearoyl−coenzyme A desaturase 1 were significantly up-regulated.[14] For mice, HFD led to systematic transcriptomic and proteomic alterations in liver including up-regulation of genes involving fatty-acid oxidation and down-regulation of genes regulating lipogenesis, selenium-binding protein 2 and glutathione *S*-transferases μ1 and π1.[15] HFD intake also enhanced the expression of pro-inflammatory cytokines and chemokines

Received: April 12, 2013
Published: May 24, 2013

accompanied with outstanding level changes in plasma adipokines including leptin, resistin, adipsin and adiponectin.[16] Furthermore, HFD significantly altered the transcriptions of several key fibrotic genes together with the pro-inflammatory cytokines and chemokines, such as disintegrin and interleukin 1 receptor antagonist, in the mouse epididymal white adipose tissue (WAT).[16] These results suggest that disorders of mammalian endogenous metabolism are closely associated with the HFD-induced obesity.

It is interesting to note that intake of prebiotics such as oligofructans (e.g., inulin) has shown functions to reduce mean daily energy-intake and weight gains.[17] Intake of inulin-type fructans also lowered blood lipids, cholesterols, epididymal fat mass[17] and triacylglycerols (TG) in liver[18] indicating its potential efficacy on obesity resistance. Such effects are probably related to the inhibition activity of inulin to the HFD-induced GPR43 overexpression and PPARγ-related adipogenesis in adipose tissues[19] affecting lipid metabolism.[20]

However, it remains unclear how HFD affects metabolism in myocardium and organs related to reproductive systems. It is also unknown whether inulin intake has any counteracting effects to these HFD-induced metabolic alterations. Metabonomic analysis ought to be the method of choice for detecting and understanding such effects since metabonomics approaches are efficient in detecting the holistic metabolic alterations of integrated biological systems related to the changes of both endogenous and environmental factors.[21,22]

Such metabonomics approaches often employ multivariate statistical methods to extract the significantly changed metabolites among all these detected with NMR and MS techniques. The metabonomics approaches have already found successful application in molecular epidemiology,[23−25] molecular phenotypings,[26−29] nutritional sciences[30,31] and in understanding the etiology of complex diseases such as diabetes,[32,33] carcinogenesis,[34,35] and inflammatory bowel diseases.[36,37] A number of metabonomics studies have been conducted to understand the obesity-associated metabolic changes in animal models.[30,38−41] However, most of such studies are focused on the metabolic feature of biofluids and liver with only few of them focused on other organs or tissues. Given the importance of obesity in the development of cardiovascular diseases[5,6] and reproductive dysfunctions,[7,8] no detailed metabonomic studies have been reported so far on the obesity-associated metabolic alterations in cardiac muscle or organs in reproductive system.

In this study, we systematically investigated the effects of HFD and inulin intake on the metabolisms of the rat myocardium and testicle tissues using NMR spectroscopy in conjunction with high-throughput data analysis. Our aims are (1) to develop an efficient and feasible method of multiple univariate data analysis (MUDA) for extracting and visualizing the significantly changed metabolites detected with NMR spectroscopy and (2) to understand the impacts of HFD and inulin intake on the metabolism of rat myocardium and testicles.

MATERIALS AND METHODS

Chemicals and Animal Diets

Methanol, $NaH_2PO_4{\cdot}2H_2O$ and $K_2HPO_4{\cdot}3H_2O$ (all analytical grade) were purchased from Sinopharm Chemical Reagent Co., Ltd. (Shanghai, China). D_2O (99.9% D) was obtained from Sigma-Aldrich, Inc. (St. Louis, MO), while sodium 3-(trimethylsilyl) [2,2,3,3-$^2H_4$] propionate (TSP) was purchased from Cambridge Isotope Laboratories, Inc. (Andover, MA). Analytical grade sodium azide (NaN_3) was obtained from Tianjin Fu Chen chemicals reagent factory (Tianjin, China). Inulin employed in this study was purchased as a powder food ingredient from Orafti (Belgium) known as OraftiGR. It is a mixture of glucosyl-(fructosyl)$_n$-fructose and (fructosyl)$_m$-fructose with an average degree of polymerization over 10. Four different diets used in this study include control diet (CD), control diet containing 10% inulin (ICD), high-fat diet (HFD) and HFD containing 10% inulin (IHFD). Formulations for CD (D12450B) and HFD (D12451, Table S1) were adapted from those of Research Diet, Inc. (New Brunswick, NJ). ICD was prepared with CD and inulin (9:1, w/w), whereas IHFD was made from HFD and inulin (9:1, w/w). All animal diets were prepared by SLAC Laboratory Animals (Shanghai, China). Phosphate buffer (PB) containing 0.001% TSP (w/v), 0.1% NaN_3 (w/v), and 50% D_2O was prepared by dissolving K_2HPO_4 and NaH_2PO_4 in water (0.15 M, pH 7.4), which was used as a solvent for NMR analysis of tissue extracts due to its good stability at low temperature.[42]

Animal Experiments and Sample Collection

All animal experiments were carried out according to the national guidelines for animal research (MOST of P. R. China, 2006) using a certified SPF facility at the Animal Experiment Center of Wuhan University (Wuhan, China). Forty-five SPF male Wistar rats (weighing 298 ± 19 g, 10-weeks old) obtained from Experimental Animal Research Center of Hubei Province (Wuhan, China) were housed in a temperature- and humidity-controlled room with a 12-h light (08:00 a.m.)/12-h dark (20:00 pm) cycle. Animals were acclimatized for two weeks with access to food and water *ad libitum* followed by an extra four-day acclimatization for all animals with the control diet (CD). Animals (weighing 377 ± 28 g) were then randomly divided into three groups (with n = 15 to reflect possible heterogeneity), namely, control, high-fat diet (HFD) and HFD plus inulin (IHFD) groups, respectively. Feeding schemes for different groups are described in Figure S1. Briefly, control group rats were fed with the CD throughout 12 weeks. HFD group was fed with CD for 5 weeks followed with HFD for another 7 weeks. IHFD group was fed with ICD for 5 weeks followed with IHFD for 7 weeks. This feeding scheme will enable the detection of any preobese changes induced by HFD. All animals were then sacrificed under isoflurane anesthesia following 12 h fasting. Heart and testicle tissue samples were collected and immediately snap-frozen with liquid nitrogen followed by storage at −80 °C until analysis. Perirenal and epididymal fats were collected and weighed for each rat as well.

Sample Preparations

Myocardium (about 80 mg) and testicle tissues (about 120 mg) were extracted separately with 600 μL precooled methanol/water (2/1) using Tissuelyzer II with 5 mm stainless steel beads (QIAGEN, Hilden, Germany) at 20 Hz for 90 s. After centrifugation (14 489*g*, 4 °C) for 10 min, the supernatants were transferred separately into individual 2 mL Eppendorf tubes for each sample. This extracting procedure was further repeated twice and the three resultant supernatants for each sample were combined and lyophilized after removal of methanol *in vacuo*. The resultant extract was then redissolved into 600 μL phosphate buffer. Following another centrifugation, the supernatant (550 μL) for each sample was transferred into a 5 mm NMR tube (Norell) for NMR analysis.

dx.doi.org/10.1021/pr400341f | J. Proteome Res. 2013, 12, 3480−3495

Table 1. Data for Perirenal and Epididymal Fat Masses from Rats Fed with Three Different Diets[a]

	weight (g)[b]			p-values[c]		
	CD	HFD	IHFD	HFD vs CD	IHFD vs HFD	IHFD vs CD
perirenal fat	14.75 ± 4.10	18.52 ± 8.22	5.32 ± 2.63	0.130	1.74×10^{-5}	5.56×10^{-8}
epididymal fat	13.54 ± 3.24	16.47 ± 7.83	4.90 ± 2.65	0.199	4.44×10^{-5}	1.80×10^{-8}

[a]CD, control diet; HFD, high-fat diet; IHFD, high-fat diet containing 10% inulin. [b]Values are expressed as mean ± SD. [c]P-values were calculated from univariate analysis.

NMR Measurements

All NMR spectra were acquired at 298 K on a Bruker AV III 600 MHz NMR spectrometer equipped with an inverse cryogenic probe (Bruker Biospin, Germany). One-dimensional ^{1}H NMR spectra were acquired using the first increment of the gradient selected NOESY pulse sequence (NOESYGPPR1D) with water presaturation during both relaxation delay (2 s) and mixing time (80 ms). The 90° pulse length was adjusted to about 10 μs for each sample and 64 transients were collected into 32 k data points with the spectral width of 12 kHz (i.e., 20 ppm). All free induction decays were zero-filled to 128 k and multiplied by an exponential function with a line-broadening factor of 1 Hz prior to Fourier transformation.

For signal assignment purposes, a series of 2D NMR spectra were acquired for selected samples and processed with similar parameters as described previously.[29,43,44] These included ^{1}H−^{1}H Total Correlation Spectroscopy (TOCSY), ^{1}H−^{1}H Correlation Spectroscopy (COSY), ^{1}H J-Resolved Spectroscopy (JRES), ^{1}H−^{13}C Heteronuclear Single Quantum Correlation (HSQC) and Heteronuclear Multiple Bond Correlation spectroscopy (HMBC).

NMR Data Processing and Multivariate Data Analysis

All spectra were phase- and baseline-corrected manually and referenced to TSP (δ0.00) with TOPSPIN software package (v3.0, Bruker Biospin, Germany). The spectral regions of δ0.2−10.0 were integrated into bins of 0.004 ppm (2.4 Hz) using AMIX package (v3.9.2, Bruker Biospin, Germany). Regions at δ4.66−5.18 were discarded to eliminate the effects of imperfect water saturation. All integrated bins were then normalized to the weight of the tissue samples, respectively, to represent the absolute concentrations for all variables (i.e., metabolites).

Multivariate data analysis was conducted for the above normalized data with SIMCA-P+ (v12.0, Umetrics, Sweden). Principal Component Analysis (PCA) was performed using the mean-centered data to monitor possible outliers. Partial Least Squares Discriminant Analysis (PLS-DA) was carried out with 7-fold cross-validation (CV) using the Pareto-scaled data as X-matrix and classification information as Y-matrix. Model quality was assessed with R^2X indicating the total explained variations and Q^2 representing the model predictability. We further performed permutation tests to ensure model validities. Orthogonal Projection to Latent Structure Discriminant Analysis (OPLS-DA)[45] was also conducted with 7-fold CV and the statistical significance of the models was tested with CV-ANOVA (with $p < 0.05$ as significant).[45]

After back-transformation,[46] loadings were generated using an in-house developed MATLAB script (V7.1, Mathworks Inc.) with each variable (or metabolite signal) color-coded by the Pearson correlation coefficient, where hot colored (e.g., red) metabolites were contributing more significantly to the intergroup differentiations than cold colored (e.g., blue) ones. Cut-off values of correlation coefficients were 0.576 and 0.602 for myocardium and testicle extracts, respectively, based on the discrimination significance ($p < 0.05$).[46]

Multiple Univariate Data Analysis (MUDA) Based on Student's t Test and Nonparametric Test

All variables (i.e., aforementioned spectral bins) from NMR profiles were regarded as independent and assessed individually about their suitability for Student's t test (normal distributions and F-test) with Shapiro-Wilk test. The assessed data were then subjected to either Student's t test or nonparametric tests as appropriate about the statistical significance in terms of their intergroup differences. For the nonparametric test, Kruskal−Wallis method was employed. To analyze all these variables in a single step, we developed a MATLAB script for MUDA which can be obtained upon request. Consequently, the univariate analysis results for intergroup differences can readily be presented as a differential-metabonome plot with p-values color-coded to all variables. Those metabolites having significant intergroup differences ($p < 0.05$) were specifically colored as red.

To further ensure the reliability of the obtained results, the characteristic and least-overlapping NMR signals for those metabolites with significant intergroup differences were individually integrated and the resultant data were subjected to further Student's t test or Kruskal−Wallis test as appropriate. Furthermore, the relative concentration changes for those metabolites showing significant intergroup differences were calculated from resonance areas,[44] i.e., $(C_{HFD} - C_{CD})/C_{CD}$, $(C_{IHFD} - C_{HFD})/C_{HFD}$ and $(C_{IHFD} - C_{CD})/C_{CD}$, where C_{CD}, C_{HFD}, and C_{IHFD} denoted the metabolite concentrations in control, HFD, and IHFD groups, respectively.

RESULTS

Effects of High-Fat Diet (HFD) and Inulin on Body-Weight, Perirenal and Epididymal Fat Masses

With control diet (CD), animals showed steady increases in their body-weights for 5 weeks, whereas rats on control diet containing inulin (ICD) showed little body-weight gains (Figure S2A). Energy intakes for ICD group were about 10−20% lower than that for CD group (Figure S2B) although inulin accounted for 10% in ICD. The ICD group also had much lower body-weight gains per unit of energy-intakes (mg/kcal) than CD group (Figure S2C), indicating the presence of inulin effects. Animals on HFD for 7 weeks also had steady body-weight gains, although no significant differences were detected for rats taking HFD and CD. In contrast, animals on inulin-containing HFD (IHFD) had little body-weight gains with markedly lower body-weights compared to both HFD and control groups (Figure S2A). However, no significant differences were observed for energy intakes between HFD and IHFD groups (Figure S2B) in most time (week 6−12), whereas the body-weight gains resulting from the same energy intakes (mg/kcal) were significantly higher in HFD group than IHFD

dx.doi.org/10.1021/pr400341f | J. Proteome Res. 2013, 12, 3480−3495

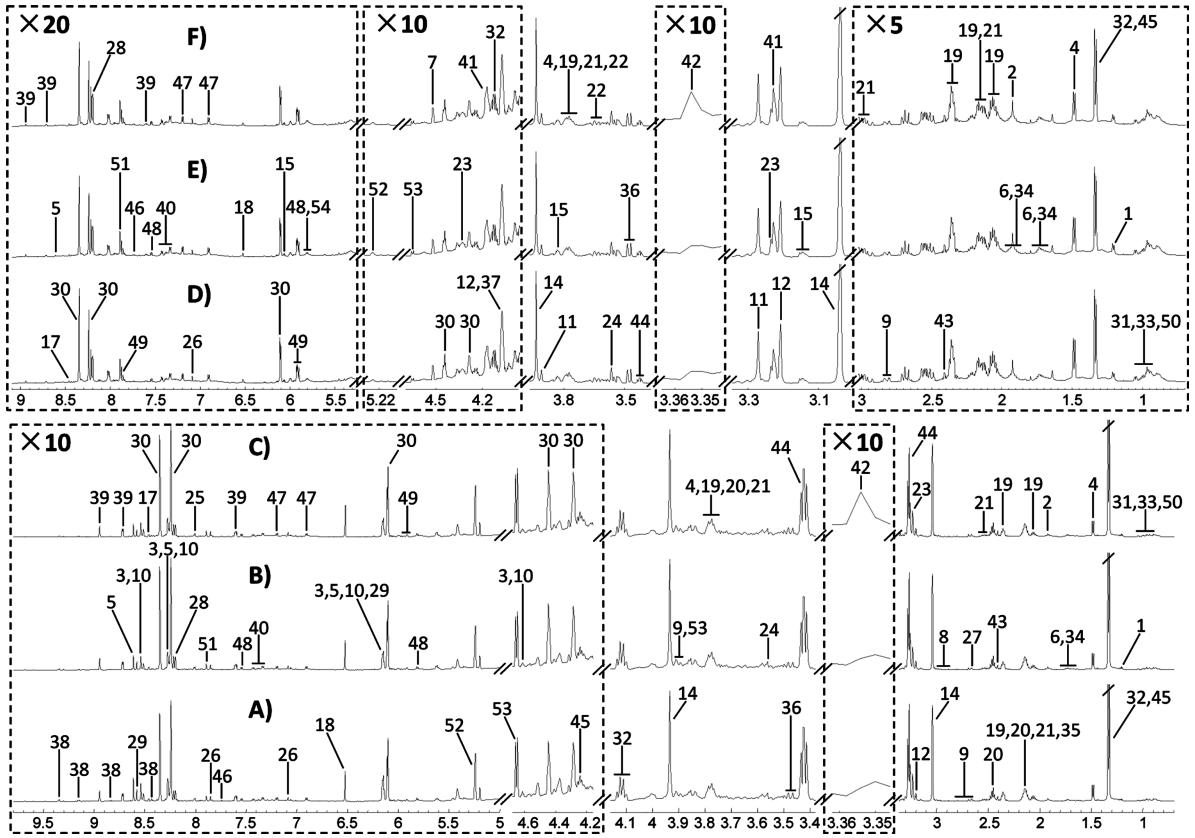

Figure 1. Average ^{1}H NMR spectra (600 MHz) for the tissue extracts of myocardium (A−C) and testicle (D−F) from rats fed with (A and D) control diet (CD), (B and E) high-fat diet (HFD) and (C and F) inulin-containing HFD (IHFD). Regions at δ3.34−3.36, 4.10−4.70 and 5.00−9.80 in A−C were vertically expanded 10 times. Regions at δ0.70−3.02 and 5.27−9.10 in D−F were vertically expanded for 5 and 20 times, respectively, whereas regions at δ3.34−3.36, 4.00−4.70 and 5.16−5.27 were expanded 10 times. Keys for metabolites are given in Table 2.

group (Figure S2C). This indicates that inulin effects are present for rats on both the control and high-fat diets.

No significant differences in both perirenal and epididymal fat masses were detected for animals in HFD and control groups, although these masses were higher in HFD group (Table 1). In contrast, such fat levels for both rat organs in the IHFD group (with inulin intake) were significantly lower than those in the HFD group. Such organ fat levels in IHFD group were even significantly lower than those in control group.

NMR Detection of Metabolites in Myocardium and Testicle Tissue Extracts

Average ^{1}H NMR spectra (Figure 1) showed rich compositional information of metabolites for the myocardium (A−C) and testicle tissue extracts (D−F) from rats fed with CD, HFD, and IHFD, respectively. Metabolites were identified with their ^{1}H and ^{13}C resonances assigned (Table 2) based on the literature data,[47−49] publically available and in-house databases. These assignments were further confirmed with a series of 2D NMR spectra. Fifty-four metabolites were identified in these tissue extracts including amino acids, carbohydrates (glucose, *myo*-inositol and *scyllo*-inositol), TCA cycle intermediates (fumarate and succinate), organic acids (lactate, formate and acetate), ketone bodies (3-hydroxybutyrate, 3-HB), purine and pyrimidine metabolites, nicotinamide, nicotinamide adenine dinucleotide (NAD^+), oxidized glutathione (GSSG), ascorbate, creatine, methyl phosphate, urea, ethanolamine, betaine, choline metabolites including choline, phosphorylcholine and glycerophosphocholine (GPC). Among them, asparagine, glutamine, hypotaurine, inosine monophosphate (IMP), adenosine diphosphate (ADP), adenosine triphosphate (ATP) and NAD^+ were detected only in myocardium extracts, whereas ascorbate, betaine, ethanolamine and urea were only found in testicle extracts. To the best of our knowledge, *scyllo*-inositol is detected in these tissues for the first time.

Visual inspection of these spectra revealed that both HFD and IHFD intake caused clear metabolite changes in both tissues as compared with controls. For instance, HFD intake resulted in level reduction for adenosine monophosphate (AMP) in myocardium tissue (Figure 1A−C), whereas inulin intake caused a remarkable elevation of *scyllo*-inositol in both myocardium and testicle extracts (Figure 1C,F). To obtain more details about the metabolite changes induced by HFD and IHFD, both multivariate data analysis (MVDA) and multiple univariate data analysis (MUDA) were conducted on these NMR data.

Multivariate Data Analysis of Myocardium and Testicle Tissue Metabolite Compositions

Multivariate analyses were conducted thoroughly for data obtained from myocardium and testicle tissue extracts including principal component analysis (PCA), PLS-DA and OPLS-DA. PCA scores plots showed no outliers for both extracts (Figures S3 and S4). However, all PLS-DA models showed low Q^2 values with poor results from the permutation tests (Figures S3 and S4). All OPLS-DA models also had low Q^2 values with *p*-values greater than 0.05 from CV-ANOVA (Figures S3 and S4). This indicates that these MVDA models are not valid or not suitable for data-mining.

dx.doi.org/10.1021/pr400341f | *J. Proteome Res.* 2013, 12, 3480−3495

Table 2. NMR Data for Metabolites Detected in Myocardium and Testicle Tissue Extracts

no.	metabolites[a]	moieties	δ^1H (multiplicity; Hz)[b]	δ^{13}C	tissues[a]
1	3-Hydroxybutyrate	C***H***$_3$	1.204(d; 6.3)	24.6	M, T
		C***H***$_2$	2.310(dd; 14.2, 6.2)	49.7	
		C***H***$_2$′	2.413(dd; 14.2, 7.4)	49.7	
		C***H***	4.160(m)	68.4	
2	Acetate	C***H***$_3$	1.929(s)	26.4	M, T
		COOH		184.0	
3	ADP	C(2)***H*** of ribose	4.613(m)	73.1	M
		C(1)***H*** of ribose	6.150(d; 5.6)	90.0	
		8-C***H*** of adenine	8.273(s)	nd	
		2-C***H*** of adenine	8.539(s)	nd	
4	Alanine	C***H***$_3$	1.488(d; 7.3)	19.6	M, T
		C***H***	3.787(m)	53.3	
		COOH		179.1	
5	AMP	C***H***$_2$	4.018(m)	66.7	M, T
		C(4)***H*** of ribose	4.370(m)	86.9	
		C(3)***H*** of ribose	4.513(m)	73.8	
		C(2)***H*** of ribose	nd	nd	
		C(1)***H*** of ribose	6.144(d; 5.9)	89.7	
		8-C***H*** of adenine	8.271(s)	155.6	
		2-C***H*** of adenine	8.613(s)	142.6	
6	Arginine	γC***H***$_2$	1.698(m)	nd	M, T
		βC***H***$_2$	1.925(m)	31.0	
		δC***H***$_2$	3.248(t; 6.9)	43.0	
		αC***H***	3.760(t)	nd	
7	Ascorbate	C***H***$_2$	3.744(m)	65.2	T
		C***H***−OH	3.966(m)	nd	
		C***H*** of the ring	4.519(d; 1.9)	81.5	
8	Asparagine	βC***H***$_2$	2.870(dd; 16.8, 7.6)	37.5	M
		βC***H***$_2$′	2.954(dd; 16.8, 4.1)	37.5	
		αC***H***	4.003(dd)	nd	
9	Aspartate	C***H***$_2$	2.683(dd; 17.4, 8.7)	39.2	M, T
		C***H***$_2$′	2.817(dd; 17.4, 3.7)	39.2	
		C***H***	3.903(dd; 8.7, 3.7)	55.1	
		COOH		179.0	
10	ATP	C(2)***H*** of ribose	4.613(m)	73.1	M
		C(1)***H*** of ribose	6.150(d; 5.6)	90.0	
		8-C***H*** of adenine	8.274(s)	nd	
		2-C***H*** of adenine	8.539(s)	nd	
11	Betaine	(C***H***$_3$)$_3$	3.270(s)	56.1	T
		C***H***$_2$	3.907(s)	68.9	
		COOH		172.1	
12	Choline	(C***H***$_3$)$_3$	3.207(s)	56.7	M, T
		NC***H***$_2$	3.517	70.6	
		C***H***$_2$OH	4.073	57.8	
13	CMP	C-C***H*** of cytosine	6.143(d; 7.6)	nd	M, TT
		N-C***H*** of cytosine	8.093(d; 7.6)	nd	
14	Creatine	C***H***$_3$	3.039(s)	39.6	M, T
		C***H***$_2$	3.935(s)	56.5	
		C═NH		159.8	
		COOH		177.1	
15	Cytidine	C(5)***H*** of ribose	4.134	87.1	M, T
		C(4)***H*** of ribose	4.237(t; 5.7)	72.4	
		C(3)***H*** of ribose	nd	nd	
		C(2)***H*** of ribose	5.913(d; 3.9)	92.8	
		N−CH═C***H***	6.069(d; 7.6)	99.6	
		N-C***H***═CH	7.850(d; 7.6)	144.8	
16	Ethanolamine	N-C***H***$_2$	3.145(t; 5.2)	44.3	T
		HO-C***H***$_2$	3.830(t; 5.2)	60.5	
17	Formate	***H***COOH	8.463(s)	172.4	M, T
18	Fumarate	C***H***	6.530(s)	138.1	M, T
		COOH		177.7	

dx.doi.org/10.1021/pr400341f | J. Proteome Res. 2013, 12, 3480−3495

Table 2. continued

no.	metabolites[a]	moieties	δ^1H (multiplicity; Hz)[b]	δ^{13}C	tissues[a]
19	Glutamate	βCH_2	2.060(m)	30.2	M, T
		βCH_2'	2.132(m)	30.2	
		γCH_2	2.354(m)	36.5	
		CH	3.763(dd; 7.3, 4.7)	57.7	
		COOH		184.3	
20	Glutamine	βCH_2	2.136(m)	29.6	M
		γCH_2	2.457(m)	34.0	
		CH	3.779(t; 6.2)	57.4	
21	GSSG	Glu βCH_2	2.165(m)	29.4	M, T
		Glu γCH_2	2.516(m)	34.4	
		Glu γCH_2'	2.563(m)	34.4	
		Cys βCH_2	2.977(dd; 14.2, 9.6)	41.7	
		Cys βCH_2'	3.314(dd; 14.2, 4.4)	41.7	
		Glu αCH	3.782(m)	57.3	
		Cys αCH	4.763(dd)	55.7	
		Gly αCH_2	nd	nd	
22	Glycerol	(CH_2)$_2$	3.566(dd; 11.7, 6.5)	65.2	M, T
		(CH_2')$_2$	3.658(dd; 11.7, 4.3)	65.2	
		CH	3.791(m)	74.7	
23	GPC	(CH_3)$_3$	3.233(s)	57.0	M, T
		CH_2−OH	3.683(m)	65.1	
		NCH_2	3.684(m)	69.1	
		OCH_2 of glycerol	3.883(m)	69.6	
		CH−OH	3.923(m)	72.7	
		OCH_2' of glycerol	3.952(m)	69.6	
		NCH$_2$CH_2	4.330(m)	62.5	
24	Glycine	CH_2	3.570(s)	44.6	M, T
		COOH		178.3	
25	Guanosine	CH of guanine	8.007(s)	141.3	M, T
26	Histidine	CH_2	3.180	nd	M, T
		CH_2'	3.264	nd	
		HOOC-CH	nd	nd	
		C═CH	7.099(d)	120.2	
		N═CH	7.896(d)	139.1	
		quaternary C		134.2	
27	Hypotaurine	CH_2-S	2.661(t; 6.9)	58.9	M
		CH_2-N	3.364(t; 6.9)	36.5	
28	Hypoxanthine	C(2)H	8.197(s)	148.5	M, T
		C(7)H	8.216(s)	144.9	
		C(9)		122.2	
		C−OH		155.1	
		C(5)		160.5	
29	IMP	CH_2	4.026(m)	65.5	M
		C(4)H of ribose	4.374(m)	87.0	
		C(3)H of ribose	4.517(dd; 5.2, 3.5)	72.8	
		C(2)H of ribose	nd	77.3	
		C(1)H of ribose	6.150(d; 5.8)	89.3	
		8-CH of hypoxanthine	8.240(s)	148.8	
		2-CH of hypoxanthine	8.578(s)	142.3	
		quaternary C		151.7	
		C═O		161.6	
30	Inosine	CH_2	3.847	64.2	M, T
		CH_2'	3.917	64.2	
		C(4)H of ribose	4.284(dd; 7.1, 3.7)	88.6	
		C(3)H of ribose	4.445(dd; 5.0, 4.0)	73.4	
		C(2)H of ribose	nd	nd	
		C(1)H of ribose	6.105(d; 5.7)	91.3	
		8-CH of hypoxanthine	8.241(s)	149.4	
		2-CH of hypoxanthine	8.351(s)	143.2	
		quaternary C		151.3	
		C═O		161.8	

dx.doi.org/10.1021/pr400341f | J. Proteome Res. 2013, 12, 3480−3495

Table 2. continued

no.	metabolites[a]	moieties	δ^1H (multiplicity; Hz)[b]	δ^{13}C	tissues[a]
31	Isoleucine	δC***H***$_3$	0.943(t; 7.4)	14.1	M, T
		βCH-C***H***$_3$	1.014(d; 7.0)	17.7	
		γC***H***$_2$	1.267(m)	27.0	
		γC***H***$_2'$	1.470(m)	27.0	
		βC***H***	1.984(m)	38.9	
		αC***H***	3.676(d; 4.0)	63.0	
		COOH		177.0	
32	Lactate	C***H***$_3$	1.338(d; 6.9)	22.6	M, T
		C***H***	4.124(q; 6.9)	71.7	
		COOH		185.4	
33	Leucine	δC***H***$_3$	0.959(d; 6.1)	24.1	M, T
		δ'C***H***$_3$	0.970(d; 6.1)	25.1	
		βC***H***$_2$	1.696(m)	42.9	
		γC***H***	1.721(m)	26.8	
		βC***H***$_2'$	1.738(m)	42.9	
		αC***H***	3.740(m)	56.5	
		COOH		117.6	
34	Lysine	γC***H***$_2$	1.454(m)	24.6	M, T
		γC***H***$_2'$	1.514(m)	24.6	
		δC***H***$_2$	1.732(m)	29.4	
		βC***H***$_2$	1.909(m)	32.9	
		εC***H***$_2$	3.030(t; 7.5)	42.2	
		C***H***	3.762	57.7	
		COOH		177.5	
35	Methionine	C***H***$_3$	2.141(s)	17.0	M, T
		βC***H***$_2$	2.202(m)	32.8	
		γC***H***$_2$	2.646(t; 7.6)	31.8	
		αC***H***	3.864(m)	56.5	
36	Methyl phosphate	C***H***$_3$	3.476(d; 10.1)	54.1	M, T
37	*myo*-Inositol	C(2)***H***	3.288(t; 9.3)	76.8	M, T
		C(4)***H***, C(6)***H***	3.543(dd; 9.9, 3.0)	74.6	
		C(1)***H***, C(3)***H***	3.629(dd; 9.9, 9.3)	75.0	
		C(5)***H***	4.073(t; 2.9)	74.5	
38	NAD^+	8-C***H*** of adenine	8.180(s)	nd	M
		5-C***H*** of nicotinamide	8.187(m)	nd	
		2-C***H*** of adenine	8.432(s)	nd	
		4-C***H*** of nicotinamide	8.834(dd)	nd	
		6-C***H*** of nicotinamide	9.143(m)	nd	
		2-C***H*** of nicotinamide	9.345(s)	nd	
39	Nicotinamide	C(5)***H***	7.604(ddd)	127.2	M, T
		C(4)***H***	8.256(ddd)	139.6	
		C(6)***H***	8.717(dd; 4.7, 1.7)	154.4	
		C(2)***H***	8.944(dd)	150.5	
		C(3)		132.2	
40	Phenylalanine	C***H***$_2$	3.131(dd; 14.5, 7.8)	39.5	M, T
		C***H2***$'$	3.284(dd; 14.5, 5.2)	39.5	
		N-C***H***	3.995(dd)	58.8	
		o-C***H***	7.334(m)	132.3	
		p-C***H***	7.381(m)	130.9	
		m-C***H***	7.432(m)	132.1	
		quaternary C		138.0	
		COOH		175.9	
41	Phosphorylcholine	(C***H***$_3$)$_3$	3.224(s)	56.7	M, T
		N-C***H***$_2$	3.593(m)	69.4	
		O-C***H***$_2$	4.176(m)	60.8	
42	*scyllo*-Inositol	$C_6H_6O_6$	3.356(s)	76.5	M, T
43	Succinate	C***H***$_2$	2.410(s)	37.1	M, T
		COOH		185.2	
44	Taurine	S-C***H***$_2$	3.275(t; 6.6)	50.4	M, T
		N-C***H***$_2$	3.432(t; 6.6)	38.3	
45	Threonine	C***H***$_3$	1.338(d; 6.8)	22.6	M, T

dx.doi.org/10.1021/pr400341f | *J. Proteome Res.* 2013, 12, 3480−3495

Table 2. continued

no.	metabolites[a]	moieties	δ^1H (multiplicity; Hz)[b]	δ^{13}C	tissues[a]
		C***H***−OH	3.597(d; 4.9)	63.3	
		C***H***-NH_2	4.258(m)	69.1	
46	Tryptophan	C(8)***H*** of indole	7.203(m)	122.3	M, T
		C(9)***H*** of indole	7.289(m)	124.9	
		C(2)***H*** of indole	7.328(s)	128.0	
		C(6)***H*** of indole	7.548(m)	115.2	
		C(7)***H*** of indole	7.741(m)	121.3	
		C(5) of indole		92.5	
47	Tyrosine	CH_2	3.061(dd; 14.7, 7.7)	38.6	M, T
		CH_2'	3.194(dd)	38.6	
		N-C***H***	3.943(dd)	59.0	
		o-C***H*** to C−OH	6.904(m)	118.7	
		m-C***H*** to C−OH	7.196(m)	133.5	
		quaternary C		129.6	
		C−OH		158.0	
		COOH		177.1	
48	Uracil	N−CH=C***H***	5.808(d; 7.7)	104.1	M, T
		N-C***H***=CH	7.548(d; 7.7)	146.6	
		C(2)=O		156.7	
49	Uridine	CH_2	3.802(dd)	64.1	M, T
		CH_2'	3.906(dd)	64.1	
		C(5)***H*** of ribose	4.137(m)	87.0	
		C(4)***H*** of ribose	4.235(dd)	72.3	
		C(3)***H*** of ribose	4.360(dd)	76.8	
		C(2)***H*** of ribose	5.904(d; 8.1)	105.4	
		C-C***H*** of uracil	5.923(d; 4.7)	92.4	
		N-C***H*** of uracil	7.883(d; 8.1)	144.8	
50	Valine	γCH_3	0.994(d; 7.0)	19.8	M, T
		γ′CH_3	1.045(d; 7.0)	21.0	
		βC***H***	2.277(m)	32.2	
		αC***H***	3.617(d; 4.3)	63.4	
		COOH		177.4	
51	Xanthine	C***H***	7.900(s)	143.6	M, T
		C(5)		112.9	
		C(9)		153.4	
52	α-Glucose	C(4)***H***	3.406	71.8	M, T
		C(2)***H***	3.588(dd; 9.7, 3.8)	74.3	
		C(3)***H***	3.733	75.1	
		CH_2	3.733	nd	
		CH_2'	3.846	64.0	
		C(5)***H***	3.846	75.3	
		C(1)***H***	5.259(d; 3.75)	95.0	
53	β-Glucose	C(2)***H***	3.294	76.9	M, T
		C(4)***H***	nd	nd	
		C(3)***H***, C(5)***H***	3.515	78.5	
		CH_2	3.743	63.6	
		CH_2'	3.909(dd; 12.3, 2.1)	63.6	
		C(1)***H***	4.656(d; 7.9)	95.0	
54	Urea	$(NH_2)_2$	5.806(br.s)		T

[a]M, myocardium; T, testicle. ADP, adenosine diphosphate; AMP, adenosine monophosphate; ATP, adenosine triphosphate; CMP, citidine monophosphate; GSSG, oxidized glutathione; GPC, glycerophosphocholine; IMP, inosine monophosphate; NAD^+, nicotinamide adenine dinucleotide. [b]s, singlet; d, doublet; t, triplet; q, quartet; m, multiplet; dd, doublet of doublets; ddd, doublet of doublets of doublets; br.s, broad singlet; nd, not determined.

However, the Student's *t* test clearly showed that *scyllo*-inositol levels were significantly different between groups with and without inulin intake. Close inspection showed that *p*-values for some OPLS-DA models were close to 0.05. Loadings plots from OPLS-DA models seemed to suggest significant intergroup differences for some metabolites (marked as red in Figures S5 and S6) in both tissue extracts.

Multiple Univariate Data Analysis of Myocardium and Testicle Tissue Metabolite Compositions

We further developed an efficient method based on classical Student's *t* test (if criteria met) or nonparametric approach to carry out univariate analysis of all variables in a single step. We generated a "differential-metabogram" plot from averaged difference-spectrum by coding all variables with their

dx.doi.org/10.1021/pr400341f | J. Proteome Res. 2013, 12, 3480−3495

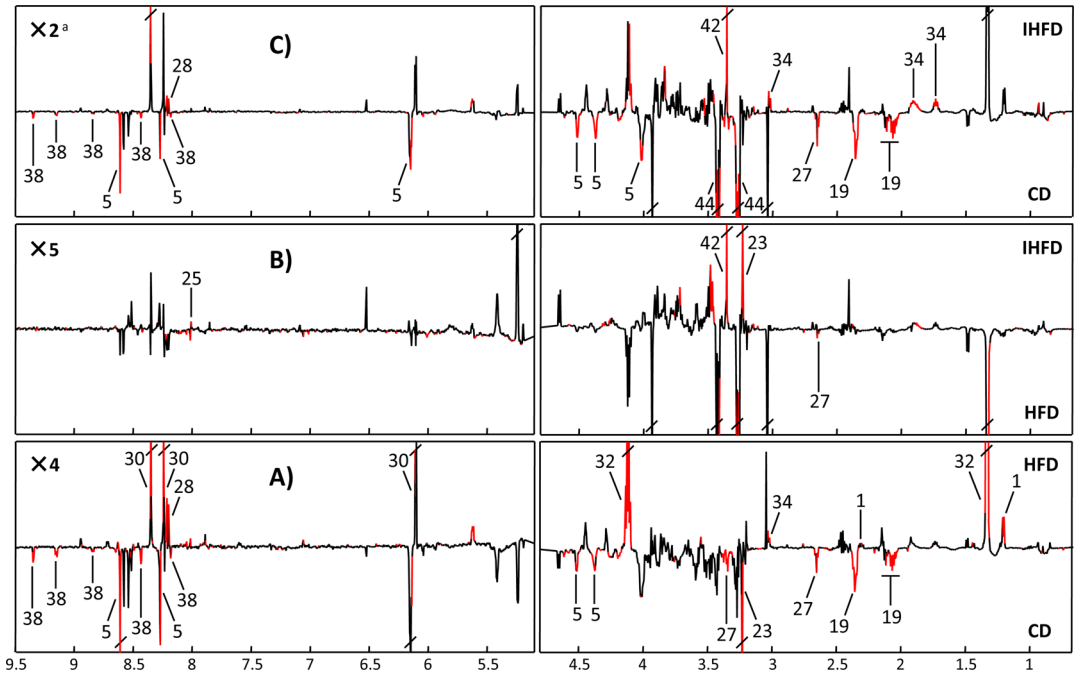

Figure 2. Differential-metabograms for myocardium tissue extracts of rats fed with control diet (CD), high-fat diet (HFD) and high-fat diet containing 10% inulin (IHFD). Metabolites with red color had significant differences. (a) Magnification factors for region at δ5.1−9.5. Keys for metabolites are given in Table 2.

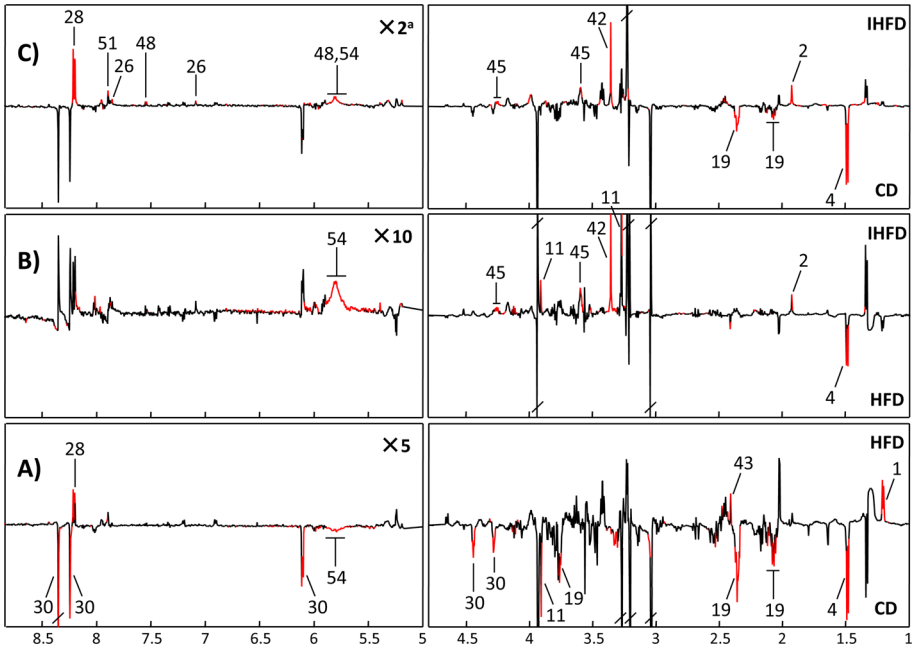

Figure 3. Differential-metabograms for testicle tissue extracts of rats fed with control diet (CD), high-fat diet (HFD) and high-fat diet containing 10% inulin (IHFD). Metabolites with red color had significant differences. (a) Magnification factors for region at δ5.0−8.8. Keys for metabolites are given in Table 2.

corresponding *p*-values obtained from Student's *t* test or Kruskal−Wallis test as appropriate. In this way, the variables (or metabolites) having significant intergroup differences were clearly revealed with *p*-values color-coded (Figures 2 and 3 and Table 3). Since *p*-values in the differential-metabograms were individually obtained for all variables, we further analyzed the peak integrals of these metabolite signals (with the least overlapping) by the Student's *t* test or Kruskal−Wallis test to verify the reliability of our method. The results (Figures S7 and S8 and Tables S2 and S3) agreed nicely with those from our MUDA. Therefore, we further analyzed the metabolic changes induced by HFD and inulin intake with our newly developed approach.

High-Fat Diet and Inulin Intake Induced Metabonomic Changes in Myocardium and Testicle Tissues

Differential-metabograms from multiple univariate data analysis (Figure 2) indicated that HFD intake for 7 weeks caused significant elevation of lysine, 3-HB, lactate, hypoxanthine and

dx.doi.org/10.1021/pr400341f | J. Proteome Res. 2013, 12, 3480−3495

Table 3. *P*-Values from Multiple Univariate Data Analysis for Metabolites in Myocardium and Testicle Tissues of Rats Fed with Three Different Diets[a]

	myocardium tissue			testicle tissue		
metabolites (keys)	HFD vs CD	IHFD vs HFD	IHFD vs CD	HFD vs CD	IHFD vs HFD	IHFD vs CD
Lysine (34)[b]	0.032		0.011			
Glutamate (19)	−0.023[c]		−0.026	−0.005		−0.006
Alanine (4)				−0.003	−0.007	−0.000
Threonine (45)					0.002	0.001
Histidine (26)						0.030
Taurine (44)			−0.020			
Hypotaurine (27)	−0.000[d]	−0.040	−0.000			
3-HB (1)	0.007			0.006		
Lactate (32)	0.003					
Succinate (43)				0.004		
Acetate (2)					0.027	0.003
scyllo-Inositol (42)		0.000	0.000		0.000	0.000
GPC (23)	−0.001	0.025				
Inosine (30)	0.012			−0.009		
Guanosine (25)		0.039				
NAD^+ (38)	−0.000		−0.014			
AMP (5)	−0.016		−0.002			
Hypoxanthine (28)	0.009		−0.041	0.011		0.006
Xanthine (51)						0.024
Betaine (11)				−0.035	0.039	
Urea (54)				−0.000	0.000	0.008
Uracil (48)						0.021

[a]CD: control diet; HFD: high-fat diet; IHFD: high-fat diet containing 10% inulin. [b]Metabolite keys are in Table 2. [c]positive and negative signs indicate the elevation and decrease of the metabolites. Values for $p \geq 0.05$ were not tabulated. [d]All values were recorded with three decimals and 0.000 meant *p*-value was less than 0.001. 3-HB, 3-hydroxybutyrate; GPC, glycerophosphocholine; AMP, adenosine monophosphate; NAD^+, nicotinamide adenine dinucleotide.

inosine accompanied with significant level decline for glutamate, hypotaurine, GPC, AMP and NAD^+ in the myocardium tissue (Table 3). In the testicle tissue, this treatment also significantly raised the levels of 3-HB, succinate and hypoxanthine but significantly lowered the levels of glutamate, alanine, betaine, inosine and urea (Figure 3). Furthermore, results from HFD and IHFD groups indicated that inulin intake caused significant changes in both tissues under HFD. In myocardium tissue, such changes were highlighted by the level elevation of *scyllo*-inositol, GPC and guanosine accompanied with decrease of hypotaurine (Figure 2). In contrast, inulin intake led to the level elevation for threonine, betaine, acetate, *scyllo*-inositol and urea together with level decrease for alanine in testicle tissue (Figure 3). Moreover, by comparing the IHFD with CD groups, we noticed that inulin intake prevented some HFD-induced metabolite changes in myocardium tissue including 3-HB, lactate, and guanosine (Figure 2); such effects can also be observed in testicle tissue for 3-HB, inosine and betaine (Figure 3).

To obtain quantitative information about the HFD and inulin effects, we calculated the ratios of intergroup metabolite changes in both tissues (Figures 4 and 5). Compared with control diet, high-fat diet led to about 20−40% decreases for hypotaurine, AMP and NAD^+ together with about 10% decreases for glutamate and GPC in myocardium tissues (Figure 4A). HFD also caused about 15−25% increases for 3-HB, lactate and hypoxanthine together with about 10% increases for lysine and inosine (Figure 4A). Under HFD, inulin intake resulted in further 15% decrease for hypotaurine whereas about 10% increases in GPC and guanosine compared with HFD alone (Figure 4B). Inulin intake also reduced the HFD-induced elevation of 3-HB, lactate, inosine and decrease of GPC (Figure 4C). Consequently, there are no significant differences for 3-HB, lactate, GPC and inosine between the IHFD and control groups (Figure 4C). It is particularly interesting to note that inulin intake (for rats in the IHFD group) led to 200−300% level increases for *scyllo*-inositol in myocardium tissues (Figure 4B,C) compared to both CD and HFD intake.

For testicle tissues, HFD intake for 7 weeks led to more than 20% level increase for 3-HB while over 10% increase for succinate and hypoxanthine compared with control diet (Figure 5A). Concurrently, levels for Ala, Glu, betaine, inosine and urea showed about 10−15% level decreases (Figure 5A). Under HFD, inulin intake induced further 10% decrease for alanine level together with about 30% level increase for urea and about 10% level increases for threonine and acetate (Figure 5B). Inulin intake prevented against the HFD-induced changes for 3-HB, succinate, betaine and inosine (Figure 5C); there were not significant differences observable anymore for the levels of four metabolites between IHFD and control goups. The most remarkable inulin-induced change was also reflected in about 200% level increase for *scyllo*-inositol in this tissue.

DISCUSSION

It is well-known that obesity is associated with the increased incidences of cardiovascular[5,6] and reproductive system diseases[7,8] by enhancing the secretion of angiotensinogen, angiotensin II and resistin. It is also well documented that inulin has beneficial effects of inhibiting obesity development under high-fat-diet (HFD) and alleviating dyslipidemia and the hepatic lipid disorders.[18,50] However, it remains unknown how

dx.doi.org/10.1021/pr400341f | J. Proteome Res. 2013, 12, 3480−3495

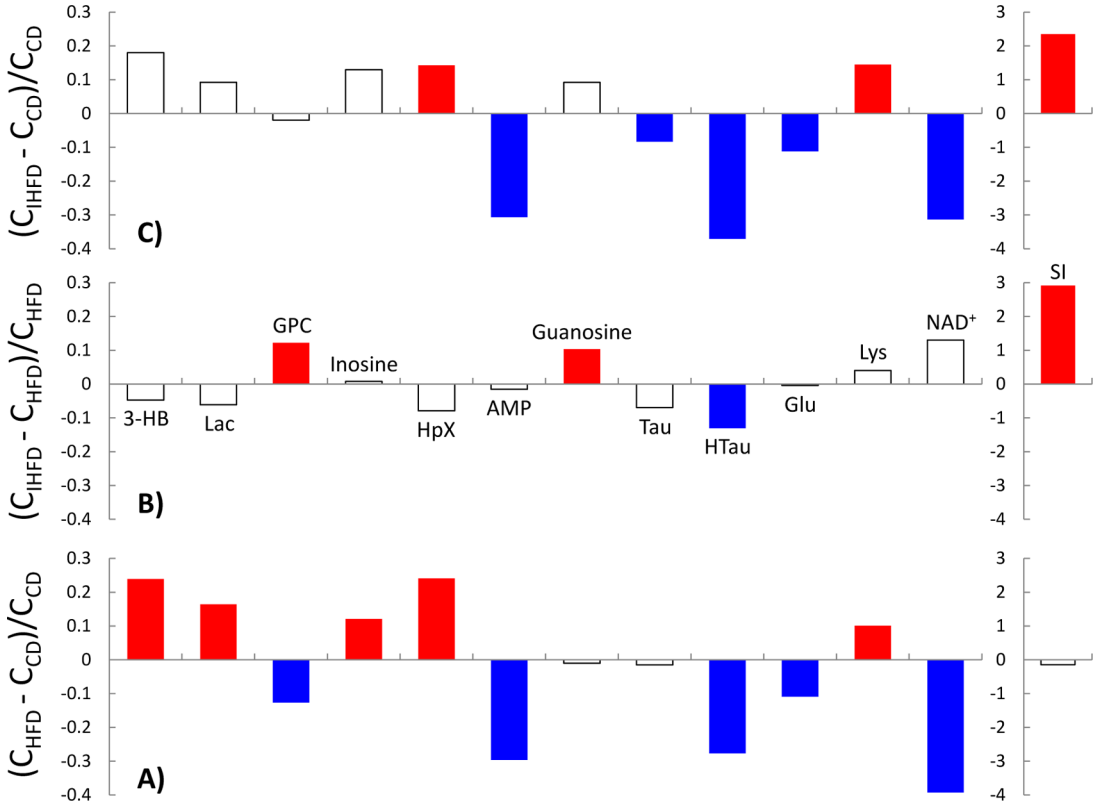

Figure 4. Relative changes for metabolite concentrations in myocardium induced by HFD (A) and inulin intake (B and C). Solid bars indicate significant changes with red for increase and blue for decrease, whereas hollow bars mean no significant changes. CD, control diet; HFD, high-fat diet; IHFD, HFD containing 10% inulin. Keys: Glu, glutamate; Lys, lysine; Tau, taurine; HTau, hypotaurine; 3-HB, 3-hydroxybutyrate; Lac, lactate; GPC, glycerophosphocholine; AMP, adenosine monophosphate; HpX, hypoxanthine; NAD^+, nicotinamide adenine dinucleotide; SI, *scyllo*-inositol.

HFD affects myocardium and testicle metabolic phenotypes or whether inulin intake has the potential to prevent obesity-induced pathogenesis of cardiovascular and male reproductive system diseases. If so, inulin intake ought to alleviate or even prevent the HFD-induced metabolic changes in myocardium and testicle tissues under HFD. Such has not been reported for the time being.

In this work, we developed a multiple univariate data analysis (MUDA) approach and investigated the effects of HFD and inulin intake on metabolic phenotypes of myocardium and testicle tissues. We found that HFD caused significant changes in rat myocardium and testicle tissues involving multiple metabolic pathways including glycolysis and fatty acid β-oxidation together with the metabolisms of choline, amino acids, purines and pyrimidines (Figure 4-5) even before HFD induced significant body-weight increase (i.e., at the preobese stage). Inulin intake prevented some HFD-induced metabolic changes in myocardium (3-HB, lactate, GPC and guanosine) and testicle tissues (3-HB, succinate, inosine and betaine) under HFD (Figure 4-5).

Phenotypic Characteristics for Rats Fed Various Diets

The observation of no significant weight gains for animals on HFD for 7 weeks (compared with those on control diet) (Figure S2A) agreed well with previous results that significant difference was observable only after HFD intake for 12 weeks.[51] Rats in HFD and control diet groups had no significant differences in both perirenal and epididymal fat masses (Table 1) though these levels were higher in HFD group. This indicated that the HFD-fed rats were in the preobese state. Inulin intake significantly inhibited the weight gains and both perirenal and epididymal fat accumulation for rats in HFD group. This is consistent with what reported[17,52,53] although animals in our study were much older and took HFD for much shorter period of time. Upon inulin intake, an immediate reduction in body-weight growth was clearly evident for rats on control diet (CD) as well and such effects continued throughout a 5-week CD-feeding (Figure S2A). Our results showed that body-weight gains per unit energy intake (mg/kcal) were significantly lower in ICD group than CD group (Figure S2C). This implies that inulin effects are significant on inhibiting body-weight gains for rats on control diet. This is broadly consistent with some previous findings resulting from oligofructose (OFS) and probably due to the OFS-induced level elevation of GLP-1, which is a key intestinal peptide involved in food intake regulations.[17,52] Inulin intake also significantly lowered the fat levels for both rat organs even with HFD (Table 1). Such organ fat levels were even significantly lower in IHFD group than those in controls (Table 1). This implies that inulin intake inhibits the accumulation of organ fats resulting from the high-fat diet as well. This is in good agreement with the previous observation that oligofructose intake can inhibit body-weight gains for rats on high-fat diet,[52] although no significant differences have been observed for the energy intakes (week 7−12) between IHFD and HFD groups (Figure S2B). This implies that inulin effects are significantly important in inhibiting body-weight gains for rats on high-fat diet apart from its satiety-promoting effects.[52]

dx.doi.org/10.1021/pr400341f | J. Proteome Res. 2013, 12, 3480−3495

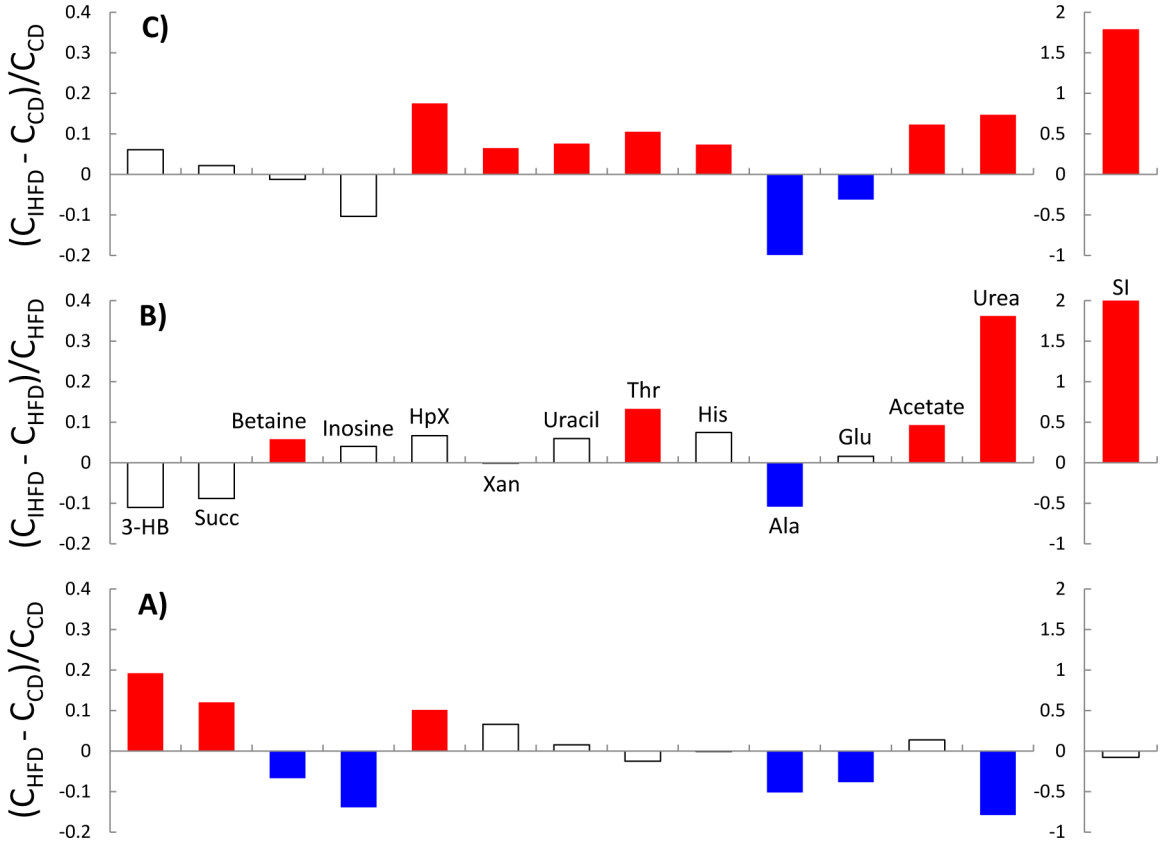

Figure 5. Relative changes for metabolite concentrations in testicle tissues induced by HFD (A) and inulin intake (B and C). Solid bars indicate significant changes with red for increase and blue for decrease, whereas hollow bars mean no significant changes. CD, control diet; HFD, high-fat diet; IHFD, HFD containing 10% inulin. CD, control diet; HFD, high-fat diet; IHFD, HFD containing 10% inulin. Keys: Ala, alanine; Glu, glutamate; Thr, threonine; His, histidine; 3-HB, 3-hydroxybutyrate; Succ, succinate; Xan, xanthine; HpX, hypoxanthine; SI, *scyllo*-inositol.

Feasibility of Multiple Univariate Data Analysis on the Metabonome

Multivariate data analysis approaches such as PCA and OPLS-DA have been widely used to extract information on the stimulus-induced metabolic changes by analyzing multiple variables simultaneously. In this study, all PLS-DA and OPLS-DA models (Figure S3−4) failed to show acceptable qualities. This is rather surprising since *scyllo*-inositol levels are clearly different between rats with inulin intake and without. The Student's *t* test further confirmed that the *scyllo*-inositol levels were significantly higher in the IHFD-fed rats than in the HFD-fed ones ($p = 9.93 \times 10^{-8}$ for myocardium; $p = 2.69 \times 10^{-10}$ for testicle tissues). Actually, *scyllo*-inositol levels in the myocardium and testicle tissues were about 200−300% higher for the IHFD-fed rats than HFD-fed ones. This suggests that PLS-DA and OPLS-DA models are more conservative and not suitable for metabonomic/metabolomic analysis when only a few variables have significant intergroup variations. Under such circumstances, univariate statistical methods are required for data analysis.

Univariate analysis of NMR data is commonly conducted using signal integrals[54] in targeted analysis. Some studies focused on untargeted metabolomics have already shown the feasibility of univariate analysis with softwares such as XCMS,[55] Metaboanalyst[56] and self-developed scripts.[57] Unfortunately, these softwares did not provide an ideal way to display the intergroup differences for significantly changed metabolites. Therefore, we developed here a method to handle all variables independently in multiple NMR spectra using the classical Student's *t* test (if criteria met) or nonparametric approach in a single step. A "differential-metabogram" was generated using the averaged difference-spectrum as a "loadings plot" with *p*-values color-coding to identify the variables (or metabolites) having significant intergroup differences (Figures 2 and 3). All results from the Student's *t* test or Kruskal−Wallis test on integrals of each metabolite signals (Figures S7 and S8 and Tables S2 and S3) showed excellent agreement with these obtained from our MUDA, thus confirming the feasibility of our method for analyzing the diet-induced metabolic changes. This also further implies that extra care has to be taken to deal with metabolomic data that simply fail multivariate modeling when PLS-DA and OPLS-DA were employed.

High-Fat Diet and Inulin Intake Induced Metabonomic Alteration in Myocardium

Metabolic changes suggested that HFD intake led to significant oxidative stresses to rat myocardium highlighted in the HFD-induced depletion of hypotaurine and NAD^+ together with elevation of 3-HB and lactate (Figure 4A). Hypotaurine (Figure 4A) is an important antioxidant[58] and an osmoregulator for myocardium whose depletion is associated with pathogenesis of the cardiovascular diseases. HFD-caused significant decrease of NAD^+ and elevation of lactate (Figure 4A) is also consistent with the HFD-enhanced fatty acid β-oxidation in rat myocardium consuming NAD^+ for transforming L-3-hydroxyacyl-CoA into 3-ketoacyl-CoA catalyzed by L-3-hydroxyacyl-CoA dehydrogenase.[59] The HFD-induced significant elevation of 3-HB (Figure 4A) is further supportive to such notion

dx.doi.org/10.1021/pr400341f | J. Proteome Res. 2013, 12, 3480−3495

although 3-HB produced in liver can also be utilized by myocardium especially when HFD elevated the ketone-body levels in rat serum.[60] HFD-induced oxidative stresses were supported by previous results on enhanced superoxide production derived from the HFD-activation of xanthine oxidase.[61] The HFD-caused concurrent elevations of myocardium inosine and hypoxanthine together with the decrease of AMP suggest (Figure 4A) the enhancement of purine catabolism. However, hypoxanthine was not oxidized further (into xanthine) probably because of insufficient supplies for NAD^+. Moreover, the HFD-induced significant decrease of rat myocardium GPC (Figure 4A) indicated that HFD caused changes in membrane metabolism with GPC as a degradation product of membrane phosphatidylcholines.

The effects of inulin intake with HFD seemed to include inhibiting accumulations of organ fats (Table 1) and ketogenesis from fatty acid oxidations. In contrast, myocardium levels for 3-HB, lactate, GPC and inosine were no longer differentiable for the IHFD and control groups (Figure 4C). This is in broad agreement with recent findings of preventative effects of inulin intake toward oxidative stress.[62] However, Inulin intake did not prevent the HFD-induced elevation of lysine and hypoxanthine together with the depletion of glutamate, AMP, NAD^+ and hypotaurine (Figure 4C). In fact, in this study, we observed a further decrease of taurine and hypotaurine by inulin addition (Figure 4B). This is probably due to the inulin-induced remarkable reductions of organ adipose tissues which have good capacity for taurine synthesis[63] with hypotaurine as an intermediate product.

It was remarkable to note that inulin intake led to about 4-fold increase for *scyllo*-inositol level (Figure 4B), which was not affected by HFD (Figure 4A). An exhaustive literature survey has shown that such observation has not been reported so far. Since *myo*-inositol is a well-known compatible osmolyte,[64] it is reasonable to propose that its isomer, *scyllo*-inositol, might also play some roles in osmotic regulation when HFD induced osmotic stresses to myocardial cells. However, there is little information available so far about biosynthesis of *scyllo*-inositol and the molecular mechanistic aspects of the inulin-induced *scyllo*-inositol elevations in mammalian myocardium.

High-Fat Diet and Inulin Intake Induced Metabonomic Alteration in Testicles

HFD caused metabolic changes in rat testicle tissues including the metabolisms of fatty acids, amino acids and purines together with TCA cycle. In testicle tissue, HFD-caused elevation of 3-HB (Figure 5A) as seen in rat myocardium indicates promotion of β-oxidation of fatty acids accompanied with accumulation of epididymal fat (Table 1). The HFD-induced elevation of succinate is in broad agreement with the previous findings that HFD down-regulates succinate dehydrogenase in rat muscle[65] and in mice liver.[66] The HFD-induced significant decreases of alanine and glutamate (Figure 5A) may be related to the HFD-caused disruptions to transamination with significant elevation of ALT.[67] Significant depletion of inosine and concurrent elevation of hypoxanthine (Figure 5A) suggested HFD-promoted purine catabolism in rat testicle as well. Decrease of betaine level in rat testicle (Figure 5A) indicated that the HFD-induced disruptions to osmotic regulation since betaine supplementation alleviated the HFD-induced hepatic pathological changes.[67]

Inulin intake had clear effects on the HFD-induced metabolic changes (Figure 5C). Under HFD, inulin intake completely prevented the HFD-induced changes in 3-HB (fatty acid β-oxidation), succinate, inosine and betaine. HFD-caused elevation of hypoxanthine together with the decreases of alanine and glutamate were not significantly affected by inulin intake. Furthermore, inulin intake resulted in elevation of threonine, histidine, xanthine, hypoxanthine and uracil compared with animals on control diet. Nevertheless, inulin-induced metabolic changes are probably associated with its effective inhibition to the accumulations of testicle adipose tissues (Table 1). Moreover, inulin-induced significant elevation of acetate in testicle is consistent with the inulin-enhanced whole-body acetate turnover[68] and probably results from colonic fermentation of inulin.[68] Inulin intake with HFD caused about 3-fold level increase for *scyllo*-inositol in rat testicle tissue (Figure 5B,C) compared with both HFD and control groups, which is surprisingly similar to what observed in rat myocardium. However, as in the case of rat myocardium, both the mechanistic and functional aspects of such *scyllo*-inositol elevation need exploring further.

CONCLUSIONS

Our high-throughput multiple univariate data analysis method was proved to be feasible and reliable for extracting statistical information on metabolites affected by diets. This method is particularly useful when only limited variables (metabolites) have significant changes so that multivariate modeling methods fail to work. We further found that even at the preobese stage, HFD caused adverse effects on the rat myocardium and testicle tissues including adipose tissue accumulation, enhanced fatty acid β-oxidation and oxidative stress, disruption to osmotic regulations and purine catabolism. The HFD-induced metabolic changes were tissue-dependent and probably attributable to obesity-associated cardiovascular and male reproductive system diseases. Inulin intake clearly ameliorated some of these adverse effects and even prevented some of them such as adipose tissue accumulation and fatty acid β-oxidation. It is particularly noticeable that inulin intake drastically increased *scyllo*-inositol levels in both tissues which may act as an osmolyte and antioxidant. However, the mechanistic aspects of its biosynthesis and potential biological functions remain to be further studied.

ASSOCIATED CONTENT

Supporting Information

Table S1, formula for control and high-fat diets; Table S2, results from the Student's *t* test (if criteria met) or Kruskal–Wallis test for some metabolites in myocardium tissues from rats; Table S3, Results from the Student's *t* test (if criteria met) or Kruskal–Wallis test for some metabolites in testicle tissues from rats; Figure S1, schematic illustrations for animal experiments; Figure S2, changes of body weights and energy intakes for rats; Figure S3, heart model evaluation; Figure S4, testicle model evaluation; Figures S5 and S6, OPLS-DA loading plots; Figure S7, results from the Student's *t* test (if criteria met) or Kruskal–Wallis test of metabolites in myocardium from rats to validate the results from the muliple univariate analysis; Figure S8, results from the Student's *t* test (if criteria met) or Kruskal–Wallis test of metabolites in testicle tissues from rats to validate the results from the multiple univariate data analysis. This material is available free of charge via the Internet at http://pubs.acs.org.

AUTHOR INFORMATION

Corresponding Author

*E-mail, Huiru.tang@wipm.ac.cn; phone,+86-27-87198430; fax, +86-27-87199291.

Notes

The authors declare no competing financial interest.

ACKNOWLEDGMENTS

We acknowledge the financial support from the Ministry of Science and Technology of China (2010CB912501 and 2012CB934004), National Natural Science Foundation of China (20825520, 21175149 and 21221064) and Chinese Academy of Sciences (KJCX2-YW-W13 and KSCX1-YW-02).

REFERENCES

(1) Ogden, C. L.; Carroll, M. D.; Kit, B. K.; Flegal, K. M. Prevalence of obesity in the United States, 2009−2010. *NCHS Data Brief.* **2012**, *82*, 1−8.

(2) Levine, J. A. Obesity in China: causes and solutions. *Chin. Med. J. (Beijing, China, Engl. Ed.)* **2008**, *121*, 1043−1050.

(3) Kotsis, V.; Stabouli, S.; Papakatsika, S.; Rizos, Z.; Parati, G. Mechanisms of obesity-induced hypertension. *Hypertens. Res.* **2010**, *33*, 386−393.

(4) Lazar, M. A. How obesity causes diabetes: Not a tall tale. *Science* **2005**, *307*, 373−375.

(5) Apovian, C. M.; Gokce, N. Obesity and cardiovascular disease. *Circulation* **2012**, *125*, 1178−1182.

(6) Kenchaiah, S.; Evans, J. C.; Levy, D.; Wilson, P. W. F.; Benjamin, E. J.; Larson, M. G.; Kannel, W. B.; Vasan, R. S. Obesity and the risk of heart failure. *N. Engl. J. Med.* **2002**, *347*, 305−313.

(7) Norman, J. E. The adverse effects of obesity on reproduction. *Reproduction* **2010**, *140*, 343−345.

(8) Du Plessis, S. S.; Cabler, S.; McAlister, D. A.; Sabanegh, E.; Agarwal, A. The effect of obesity on sperm disorders and male infertility. *Nat. Rev. Urol.* **2010**, *7*, 153−161.

(9) Backhed, F.; Ding, H.; Wang, T.; Hooper, L. V.; Koh, G. Y.; Nagy, A.; Semenkovich, C. F.; Gordon, J. I. The gut microbiota as an environmental factor that regulates fat storage. *Proc. Natl. Acad. Sci. U.S.A.* **2004**, *101*, 15718−15723.

(10) Oh, D. Y.; Olefsky, J. M. Wnt fans the flames in obesity. *Science* **2010**, *329*, 397−398.

(11) Shai, I.; Schwarzfuchs, D.; Henkin, Y.; Shahar, D. R.; Witkow, S.; Greenberg, I.; Golan, R.; Fraser, D.; Bolotin, A.; Vardi, H.; Tangi-Rozental, O.; Zuk-Ramot, R.; Sarusi, B.; Brickner, D.; Schwartz, Z.; Sheiner, E.; Marko, R.; Katorza, E.; Thiery, J.; Fiedler, G. M.; Bluher, M.; Stumvoll, M.; Stampfer, M. J. Weight loss with a low-carbohydrate, Mediterranean, or low-fat diet. *N. Engl. J. Med.* **2008**, *359*, 229−241.

(12) Jakicic, J. M.; Marcus, B. H.; Gallagher, K. I.; Napolitano, M.; Lang, W. Effect of exercise duration and intensity on weight loss in overweight, sedentary women - A randomized trial. *JAMA, J. Am. Med. Assoc.* **2003**, *290*, 1323−1330.

(13) Rosini, T. C.; da Silva, A. S. R.; de Moraes, C. Diet-induced obesity: Rodent model for the study of obesity-related disorders. *Rev. Assoc. Med. Bras.* **2012**, *58*, 383−387.

(14) Xie, Z. Q.; Li, H. K.; Wang, K.; Lin, J. C.; Wang, Q.; Zhao, G. P.; Jia, W.; Zhang, Q. H. Analysis of transcriptome and metabolome profiles alterations in fatty liver induced by high-fat diet in rat. *Metab., Clin. Exp.* **2010**, *59*, 554−560.

(15) Kirpich, I. A.; Gobejishvili, L. N.; Homme, M. B.; Waigel, S.; Cave, M.; Arteel, G.; Barve, S. S.; McClain, C. J.; Deaciuc, I. V. Integrated hepatic transcriptome and proteome analysis of mice with high-fat diet-induced nonalcoholic fatty liver disease. *J. Nutr. Biochem.* **2011**, *22*, 38−45.

(16) Kwon, E. Y.; Shin, S. K.; Cho, Y. Y.; Jung, U. J.; Kim, E.; Park, T.; Park, J. H. Y.; Yun, J. W.; McGregor, R. A.; Park, Y. B.; Choi, M. S. Time-course microarrays reveal early activation of the immune transcriptome and adipokine dysregulation leads to fibrosis in visceral adipose depots during diet-induced obesity. *BMC Genomics* **2012**, *13*, 450−465.

(17) Delzenne, N. M.; Cani, P. D.; Daubioul, C.; Neyrinck, A. M. Impact of inulin and oligofructose on gastrointestinal peptides. *Br. J. Nutr.* **2005**, *93*, S157−S161.

(18) Letexier, D.; Diraison, F.; Beylot, M. Addition of inulin to a moderately high-carbohydrate diet reduces hepatic lipogenesis and plasma triacylglycerol concentrations in humans. *Am. J. Clin. Nutr.* **2003**, *77*, 559−564.

(19) Dewulf, E. M.; Cani, P. D.; Neyrinck, A. M.; Possemiers, S.; Van Holle, A.; Muccioli, G. G.; Deldicque, L.; Bindels, L. B.; Pachikian, B. D.; Sohet, F. M.; Mignolet, E.; Francaux, M.; Larondelle, Y.; Delzenne, N. M. Inulin-type fructans with prebiotic properties counteract GPR43 overexpression and PPAR gamma-related adipogenesis in the white adipose tissue of high-fat diet-fed mice. *J. Nutr. Biochem.* **2011**, *22*, 712−722.

(20) Delzenne, N. M.; Kok, N. Effects of fructans-type prebiotics on lipid metabolism. *Am. J. Clin. Nutr.* **2001**, *73*, 456S−458S.

(21) Tang, H. R.; Wang, Y. L. Metabonomics: A revolution in progress. *Prog. Biochem. Biophys.* **2006**, *33*, 401−417.

(22) Nicholson, J. K.; Lindon, J. C.; Holmes, E. 'Metabonomics': Understanding the metabolic responses of living systems to pathophysiological stimuli via multivariate statistical analysis of biological NMR spectroscopic data. *Xenobiotica* **1999**, *29*, 1181−1189.

(23) Teague, C.; Holmes, E.; Maibaum, E.; Nicholson, J.; Tang, H. R.; Chan, Q. N.; Elliott, P.; Wilson, I. Ethyl glucoside in human urine following dietary exposure: Detection by ^{1}H NMR spectroscopy as a result of metabonomic screening of humans. *Analyst* **2004**, *129*, 259−264.

(24) Holmes, E.; Loo, R. L.; Cloarec, O.; Coen, M.; Tang, H. R.; Maibaum, E.; Bruce, S.; Chan, Q.; Elliott, P.; Stamler, J.; Wilson, I. D.; Lindon, J. C.; Nicholson, J. K. Detection of urinary drug metabolite (Xenometabolome) signatures in molecular epidemiology studies via statistical total correlation (NMR) spectroscopy. *Anal. Chem.* **2007**, *79*, 2629−2640.

(25) Holmes, E.; Loo, R. L.; Stamler, J.; Bictash, M.; Yap, I. K. S.; Chan, Q.; Ebbels, T.; De Iorio, M.; Brown, I. J.; Veselkov, K. A.; Daviglus, M. L.; Kesteloot, H.; Ueshima, H.; Zhao, L. C.; Nicholson, J. K.; Elliott, P. Human metabolic phenotype diversity and its association with diet and blood pressure. *Nature* **2008**, *453*, 396−400.

(26) Smith, L. M.; Maher, A. D.; Want, E. J.; Elliott, P.; Stamler, J.; Hawkes, G. E.; Holmes, E.; Lindon, J. C.; Nicholson, J. K. Large-scale human metabolic phenotyping and molecular epidemiological studies-via ^{1}H NMR spectroscopy of urine: Investigation of borate preservation. *Anal. Chem.* **2009**, *81*, 4847−4856.

(27) Nicholson, J. K. Global systems biology, personalized medicine and molecular epidemiology. *Mol. Syst. Biol.* **2006**, *2*, 52.

(28) Mirnezami, R.; Kinross, J. M.; Vorkas, P. A.; Goldin, R.; Holmes, E.; Nicholson, J.; Darzi, A. Implementation of molecular phenotyping approaches in the personalized surgical patient journey. *Ann. Surg.* **2012**, *255*, 881−889.

(29) Dai, H.; Xiao, C.; Liu, H.; Hao, F.; Tang, H. Combined NMR and LC-DAD-MS analysis reveals comprehensive metabonomic variations for three phenotypic cultivars of Salvia Miltiorrhiza Bunge. *J. Proteome Res.* **2010**, *9*, 1565−1578.

(30) He, Q. H.; Ren, P. P.; Kong, X. F.; Wu, Y. N.; Wu, G. Y.; Li, P.; Hao, F. H.; Tang, H. R.; Blachier, F.; Yin, Y. L. Comparison of serum metabolite compositions between obese and lean growing pigs using an NMR-based metabonomic approach. *J. Nutr. Biochem.* **2012**, *23*, 133−139.

(31) Tang, H. R.; Wang, Y. L. In *Nutrimetabonomics: Metabonomics in Food Science*; Farhat, I. A., Belton, P. S., Webb, G. A., Eds.; Royal Society of Chemistry: London, 2007; Vol. *310*, pp 26−35.

(32) Zhang, X. Y.; Wang, Y. L.; Hao, F. H.; Zhou, X. H.; Han, X. Y.; Tang, H. R.; Ji, L. N. Human serum metabonomic analysis reveals progression axes for glucose intolerance and insulin resistance statuses. *J. Proteome Res.* **2009**, *8*, 5188−5195.

(33) Xu, W. X.; Wu, J. F.; An, Y. P.; Xiao, C. N.; Hao, F. H.; Liu, H. B.; Wang, Y. L.; Tang, H. R. Streptozotocin-induced dynamic metabonomic changes in rat biofluids. *J. Proteome Res.* **2012**, *11*, 3423−3435.
(34) Yang, Y. X.; Li, C. L.; Nie, X.; Feng, X. S.; Chen, W. X.; Yue, Y.; Tang, H. R.; Deng, F. Metabonomic studies of human hepatocellular carcinoma using high-resolution magic-angle spinning ^{1}H NMR spectroscopy in conjunction with multivariate data analysis. *J. Proteome Res.* **2007**, *6*, 2605−2614.
(35) Chen, W. X.; Lou, H. Y.; Zhang, H. P.; Nie, X.; Xiang, Y.; Yang, Y. X.; Wu, G. Y.; Qi, J. P.; Yue, Y.; Lei, H.; Tang, H. R.; Deng, F. Metabonomic characterization of the low-grade human astrocytomas and meningiomas using magic-angle spinning ^{1}H nuclear magnetic resonance spectroscopy and principal component analysis. *Prog. Biochem. Biophys.* **2008**, *35*, 1142−1153.
(36) Bjerrum, J. T.; Nielsen, O. H.; Hao, F. H.; Tang, H. R.; Nicholson, J. K.; Wang, Y. L.; Olsen, J. Metabonomics in ulcerative colitis: Diagnostics, biomarker identification, and insight into the pathophysiology. *J. Proteome Res.* **2010**, *9*, 954−962.
(37) Schicho, R.; Shaykhutdinov, R.; Ngo, J.; Nazyrova, A.; Schneider, C.; Panaccione, R.; Kaplan, G. G.; Vogel, H. J.; Storr, M. Quantitative metabolomic profiling of serum, plasma, and urine by ^{1}H NMR spectroscopy discriminates between patients with inflammatory bowel disease and healthy individuals. *J. Proteome Res.* **2012**, *11*, 3344−3357.
(38) Duggan, G. E.; Hittel, D. S.; Hughey, C. C.; Weljie, A.; Vogel, H. J.; Shearer, J. Differentiating short- and long-term effects of diet in the obese mouse using ^{1}H-nuclear magnetic resonance metabolomics. *Diabetes Obes. Metab.* **2011**, *13*, 859−862.
(39) Mestdagh, R.; Dumas, M. E.; Rezzi, S.; Kochhar, S.; Holmes, E.; Claus, S. P.; Nicholson, J. K. Gut microbiota modulate the metabolism of brown adipose tissue in mice. *J. Proteome Res.* **2012**, *11*, 620−630.
(40) Kim, I. Y.; Jung, J.; Jang, M.; Ahn, Y. G.; Shin, J. H.; Choi, J. W.; Sohn, M. R.; Shin, S. M.; Kang, D. G.; Lee, H. S.; Bae, Y. S.; Ryu, D. H.; Seong, J. K.; Hwang, G. S. ^{1}H NMR-based metabolomic study on resistance to diet-induced obesity in AHNAK knock-out mice. *Biochem. Biophys. Res. Commun.* **2010**, *403*, 428−434.
(41) Li, H.; Xie, Z.; Lin, J.; Song, H.; Wang, Q.; Wang, K.; Su, M.; Qiu, Y.; Zhao, T.; Song, K.; Wang, X.; Zhou, M.; Liu, P.; Zhao, G.; Zhang, Q.; Jia, W. Transcriptomic and metabonomic profiling of obesity-prone and obesity-resistant rats under high fat diet. *J. Proteome Res.* **2008**, *7*, 4775−4783.
(42) Xiao, C. N.; Hao, F. H.; Qin, X. R.; Wang, Y. L.; Tang, H. R. An optimized buffer system for NMR-based urinary metabonomics with effective pH control, chemical shift consistency and dilution minimization. *Analyst* **2009**, *134*, 916−925.
(43) Dai, H.; Xiao, C.; Liu, H.; Tang, H. Combined NMR and LC-MS analysis reveals the metabonomic changes in Salvia miltiorrhiza Bunge induced by water depletion. *J. Proteome Res.* **2010**, *9*, 1460−1475.
(44) Xiao, C. N.; Dai, H.; Liu, H. B.; Wang, Y. L.; Tang, H. R. Revealing the metabonomic variation of rosemary extracts using ^{1}H NMR spectroscopy and multivariate data analysis. *J. Agric. Food Chem.* **2008**, *56*, 10142−10153.
(45) Eriksson, L.; Trygg, J.; Wold, S. CV-ANOVA for significance testing of PLS and OPLS (R) models. *J. Chemometr.* **2008**, *22*, 594−600.
(46) Cloarec, O.; Dumas, M. E.; Trygg, J.; Craig, A.; Barton, R. H.; Lindon, J. C.; Nicholson, J. K.; Holmes, E. Evaluation of the orthogonal projection on latent structure model limitations caused by chemical shift variability and improved visualization of biomarker changes in ^{1}H NMR spectroscopic metabonomic studies. *Anal. Chem.* **2005**, *77*, 517−526.
(47) Fan, T. W. M.; Lane, A. N. Structure-based profiling of metabolites and isotopomers by NMR. *Prog. Nucl. Magn. Reson. Spectrosc.* **2008**, *52*, 69−117.
(48) Martin, F. P. J.; Sprenger, N.; Yap, I. K. S.; Wang, Y. L.; Bibiloni, R.; Rochat, F.; Rezzi, S.; Cherbut, C.; Kochhar, S.; Lindon, J. C.; Holmes, E.; Nicholson, J. K. Panorganismal gut microbiome-host metabolic crosstalk. *J. Proteome Res.* **2009**, *8*, 2090−2105.
(49) Martin, F. P. J.; Dumas, M. E.; Wang, Y. L.; Legido-Quigley, C.; Yap, I. K. S.; Tang, H. R.; Zirah, S.; Murphy, G. M.; Cloarec, O.; Lindon, J. C.; Sprenger, N.; Fay, L. B.; Kochhar, S.; van Bladeren, P.; Holmes, E.; Nicholson, J. K. A top-down systems biology view of microbiome-mammalian metabolic interactions in a mouse model. *Mol. Syst. Biol.* **2007**, *3*, 112−127.
(50) Parnell, J. A.; Reimer, R. A. Effect of prebiotic fibre supplementation on hepatic gene expression and serum lipids: a dose-response study in JCR:LA-cp rats. *Br. J. Nutr.* **2010**, *103*, 1577−1584.
(51) Da Silva, A. S. R.; Pauli, J. R.; Ropelle, E. R.; Oliveira, A. G.; Cintra, D. E.; De Souza, C. T.; Velloso, L. A.; Carvalheira, J. B. C.; Saad, M. J. A. Exercise intensity, inflammatory signaling, and insulin resistance in obese rats. *Med. Sci. Sports Exercise* **2010**, *42*, 2180−2188.
(52) Cani, P. D.; Neyrinck, A. M.; Maton, N.; Delzenne, N. M. Oligofructose promotes satiety in rats fed a high-fat diet: Involvement of glucagon-like peptide-1. *Obes. Res.* **2005**, *13*, 1000−1007.
(53) Kok, N. N.; Taper, H. S.; Delzenne, N. M. Oligofructose modulates lipid metabolism alterations induced by a fat-rich diet in rats. *J. Appl. Toxicol.* **1998**, *18*, 47−53.
(54) Pechlivanis, A.; Kostidis, S.; Saraslanidis, P.; Petridou, A.; Tsalis, G.; Mougios, V.; Gika, H. G.; Mikros, E.; Theodoridis, G. A. ^{1}H NMR-based metabonomic investigation of the effect of two different exercise sessions on the metabolic fingerprint of human urine. *J. Proteome Res.* **2010**, *9*, 6405−6416.
(55) Tautenhahn, R.; Patti, G. J.; Rinehart, D.; Siuzdak, G. XCMS online: A web-based platform to process untargeted metabolomic data. *Anal. Chem.* **2012**, *84*, 5035−5039.
(56) Xia, J. G.; Mandal, R.; Sinelnikov, I. V.; Broadhurst, D.; Wishart, D. S. MetaboAnalyst 2.0—a comprehensive server for metabolomic data analysis. *Nucleic Acids Res.* **2012**, *40*, W127−W133.
(57) Le Gall, G.; Puaud, M.; Colquhoun, I. J. Discrimination between orange juice and pulp wash by ^{1}H nuclear magnetic resonance spectroscopy: Identification of marker compounds. *J. Agric. Food Chem.* **2001**, *49*, 580−588.
(58) Sakuragawa, T.; Hishiki, T.; Ueno, Y.; Ikeda, S.; Soga, T.; Yachie-Kinoshita, A.; Kajimura, M.; Suematsu, M. Hypotaurine is an energy-saving hepatoprotective compound against ischemia-reperfusion injury of the rat liver. *J. Clin. Biochem. Nutr.* **2010**, *46*, 126−134.
(59) Norseth, J.; Thomassen, M. S. Stimulation of microperoxisomal beta-oxidation in rat heart by high-fat diets. *Biochim. Biophys. Acta* **1983**, *751*, 312−320.
(60) Bielohuby, M.; Menhofer, D.; Kirchner, H.; Stoehr, B. J. M.; Muller, T. D.; Stock, P.; Hempel, M.; Stemmer, K.; Pfluger, P. T.; Kienzle, E.; Christ, B.; Tschop, M. H.; Bidlingmaier, M. Induction of ketosis in rats fed low-carbohydrate, high-fat diets depends on the relative abundance of dietary fat and protein. *Am. J. Physiol.: Endocrinol. Metab.* **2011**, *300*, E65−E76.
(61) Erdei, N.; Toth, A.; Pasztor, E. T.; Papp, Z.; Edes, I.; Koller, A.; Bagi, Z. High-fat diet-induced reduction in nitric oxide-dependent arteriolar dilation in rats: Role of xanthine oxidase-derived superoxide anion. *Am. J. Physiol.: Heart Circ. Physiol.* **2006**, *291*, H2107−H2115.
(62) Stoyanova, S.; Geuns, J.; Hideg, E.; Van Den Ende, W. The food additives inulin and stevioside counteract oxidative stress. *Int. J. Food. Sci. Nutr.* **2011**, *62*, 207−214.
(63) Ueki, I.; Stipanuk, M. H. 3T3-L1 adipocytes and rat adipose tissue have a high capacity for taurine synthesis by the cysteine dioxygenase/cysteinesulfinate decarboxylase and cysteamine dioxygenase pathways. *J. Nutr.* **2009**, *139*, 207−214.
(64) Burg, M. B. Molecular basis of osmotic regulation. *Am. J. Physiol.* **1995**, *268*, F983−F996.
(65) Sparks, L. M.; Xie, H.; Koza, R. A.; Mynatt, R.; Hulver, M. W.; Bray, G. A.; Smith, S. R. A high-fat diet coordinately downregulates genes required for mitochondrial oxidative phosphorylation in skeletal muscle. *Diabetes* **2005**, *54*, 1926−1933.
(66) Eccleston, H. B.; Andringa, K. K.; Betancourt, A. M.; King, A. L.; Mantena, S. K.; Swain, T. M.; Tinsley, H. N.; Nolte, R. N.; Nagy, T.

R.; Abrams, G. A.; Bailey, S. M. Chronic exposure to a high-fat diet induces hepatic steatosis, impairs nitric oxide bioavailability, and modifies the mitochondrial proteome in mice. *Antioxid. Redox Signaling* **2011**, *15*, 447−459.
(67) Wang, Z. G.; Yao, T.; Pini, M.; Zhou, Z. X.; Fantuzzi, G.; Song, Z. Y. Betaine improved adipose tissue function in mice fed a high-fat diet: A mechanism for hepatoprotective effect of betaine in nonalcoholic fatty liver disease. *Am. J. Physiol.: Gastrointest. Liver Physiol.* **2010**, *298*, G634−G642.
(68) Pouteau, E.; Frenais, R.; Dumon, H.; Noah, L.; Martin, L.; Nguyen, P. Colonic fermentation of inulin increases whole-body acetate turnover in dogs. *J. Nutr.* **2005**, *135*, 2845−2851.